Journal of Materials Chemistry C

Accepted Manuscript

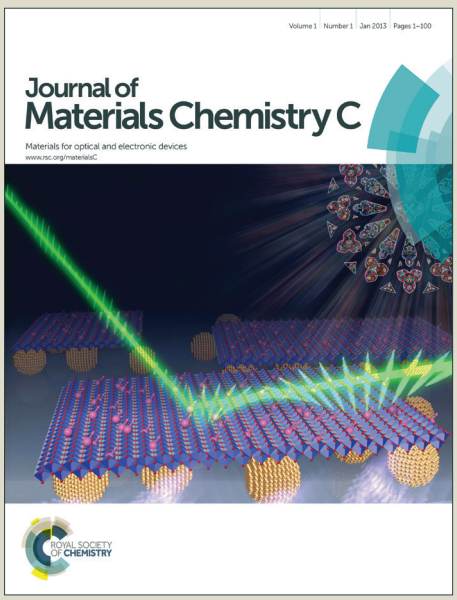

This is an *Accepted Manuscript*, which has been through the Royal Society of Chemistry peer review process and has been accepted for publication.

Accepted Manuscripts are published online shortly after acceptance, before technical editing, formatting and proof reading. Using this free service, authors can make their results available to the community, in citable form, before we publish the edited article. We will replace this *Accepted Manuscript* with the edited and formatted *Advance Article* as soon as it is available.

You can find more information about *Accepted Manuscripts* in the Information for Authors.

Please note that technical editing may introduce minor changes to the text and/or graphics, which may alter content. The journal's standard Terms & Conditions and the Ethical guidelines still apply. In no event shall the Royal Society of Chemistry be held responsible for any errors or omissions in this *Accepted Manuscript* or any consequences arising from the use of any information it contains.

ROYAL SOCIETY OF CHEMISTRY

www.rsc.org/materialsC

Journal Name

RSCPublishing

ARTICLE

Hybrids based on lanthanide ions activated yttrium metal organic frameworks: functional assembly, polymer film preparation and luminescence tuning

Cite this: DOI: 10.1039/x0xx00000x

Received 00th January 2012,
Accepted 00th January 2012

DOI: 10.1039/x0xx00000x

www.rsc.org/

Tian-Wei Duan and Bing Yan*

A series of hybrids based on lanthanide ions (Eu^{3+}, Tb^{3+}, Sm^{3+}, Dy^{3+}) activated yttrium metallic organic framework of 1,3,5-benzenetricarboxylate (MOF-76(Y)) have been synthesized by ion substitution under solvothermal conditions, which shows isostructure with parent MOF-76(Y). Meanwhile, nanoscaled MOF-76(Y): Ln (Ln = Eu, Tb, Sm, Dy) can also be prepared with assistance of moderate reagent. Structure, composition and morphology of resulting materials are characterized by XRD, EDX, and SEM. Photophysical properties of these hybrid systems are investigated in details and reveal that characteristic emission of corresponding Ln^{3+} ion is under ultraviolet radiation. In further study, the tunable emitting color of Eu^{3+} and Tb^{3+} co-activated MOF-76(Y) (x mol% Eu^{3+}: y mol% Tb^{3+} = 1: 10, 5: 10, 10: 10, 10: 5, 10: 1) are discussed. The result indicates that the tunable optical properties of MOF-76(Y): Eu/Tb depend on the concentration of activated ions and excitation wavelength. Besides, the polymer films, which are made of nanosized MOF-76(Y): Ln (Ln = Eu, Tb, Sm, Dy), are prepared in order to extend the potential application of optical device.

1. Introduction

Metal organic frameworks (MOFs) has been attracted much attention for their variety applications, such as gas storage[1], drug delivery[2], chemical sensors[3] and catalysis[4], which are result from the variety composition of binding ligands and metal centers. In recent years, fluorescent MOFs raise a great interest for their potential applications as molecule sensors[5], lighting devices[6], and biological imaging[7]. There are several ways to generate MOFs' fluorescence[8]. Highly conjugated organic linkers may give pure intra-ligand emission, metal to ligand charge transfer (MLCT) emission, or ligand to metal charge transfer (LMCT) emission. In addition, lanthanide as framework ions emit sharp but weak luminescence, however, luminescence intensity can be increased by antenna effect. The entrapped guest luminescent molecules can also confer luminescent properties onto MOFs, including exciplex formation. In decades, lanthanide metal organic frameworks (LnMOFs) are studied widely not only for their traditional utilities as gas absorption material and catalyst[9], but also for their promising potential utilities in such fields as luminescent labels, photovoltaic devices, and high-technology optics, *etc*[10]. Some novel methods are explored to synthesize nano-LnMOFs[11], whose nanoscale is of great importance to produce interesting functional nanomaterial for physical and biological applications. It needs to be referred that the potential application of LnMOFs becomes attractive for their virtues of high colour purity, high luminescence quantum efficiencies and a wide range of lifetime. Unfortunately, the application of LnMOFs is hindered by poor physical stability and low mechanical strength. In order to overcome this shortcoming, one solution is to immobilize LnMOFs in stable matrices, like polymers, ionic liquid, silicon materials, *etc*[12,13]. Embedding LnMOFs into a polymer can lead to novel transparent organic-inorganic hybrid materials, which can find potential applications in the field of optical devices such as lenses, filters and polarizers.

To date, various LnMOFs have been synthesized with different organic linkers. It is well known that benzenetricarboxylates are widely used in the construction of three-dimensional lanthanide coordination compounds, because oxygen atoms on the carboxylate can act as bridge linking to metal ions in various coordinating modes[14]. Since Yaghi group synthesized MOF-76[15], in which Tb atoms are bridged by 1,3,5-benzenetricarboxylates organic linkers to form a 3D rod-packing structure, some analogue material on the basis of lanthanide and 1,3,5-benzenetricarboxylates are synthesized later[16]. One of the important applications of MOF-76 (or its isostructural MOFs) is chemical sensor such as anion sensor[17a] or small molecule sensor[16b,17b]. Recently, Sun and cowokers[17c] also find MOF-76 can play a key role in uranium (VI) sorption. As far as we know, most reported applications of MOF-76 and

Journal of Materials Chemistry C Accepted Manuscript

its derivatives is focused on gas sorption and chemical sensing, while examples with luminescence tuning have been rarely reported. Few years ago, You and coworkers[16a] realize the synthesis of color-tunable Eu^{3+} and Tb^{3+} co-doped MOF-76 on a large amount via simple one-step precipitation method. This demonstrate that 1,3,5-benzenetricarboxylates will be a good candidate to sensitise Eu^{3+} and Tb^{3+} luminescence.

Among the lanthanide ions, Y^{3+} ions based compounds are usually used as matrices for traditional fluorescent powders, while Eu^{3+}, Tb^{3+}, Sm^{3+}, Dy^{3+} ions act as important activators. Herein we present the rare example of microporous Y(1,3,5-BTC)(nH_2O) as matrix, which make use of Y as center metal and benzenetricarboxylic acid (H_3BTC) as linker, lanthanide ions (Eu^{3+}, Tb^{3+}, Sm^{3+}, Dy^{3+}) as activators to obtain a series of luminescent lanthanide metal organic frameworks. The colour-tunable luminescence of these hybrids MOF systems were realized by adjusting doping concentration ratio of lanthanide ions or varying excitation wavelength. The polymer films based on them are also prepared for the purpose of extending application fields.

2. Experimental Section

Reagents. 1,3,5-Benzenetricarboxylic acid (H_3BTC), N,N-dimethylformamide (DMF), benzoyl peroxide (BPO), tetrahydrofuran (THF) and ethyl methacrylate (EMA) were purchased from Aldrich and used without further purification. $Y(NO_3)_3{\cdot}6H_2O$, $Eu(NO_3)_3{\cdot}6H_2O$, $Tb(NO_3)_3{\cdot}6H_2O$, $Sm(NO_3)_3{\cdot}6H_2O$ and $Dy(NO_3)_3{\cdot}6H_2O$ were prepared by dissolving their corresponding oxides in concentrated nitrate acid followed by evaporation.

Synthesis of MOF-76(Y). As a typical synthesis of Y(1,3,5-BTC)(nH_2O), $Y(NO_3){\cdot}6H_2O$ (0.107 g, 0.28 mmol) and H_3BTC (0.020 g, 0.10 mmol) were dissolved in DMF (4 mL) and H_2O (3.2 mL) at room temperature. The mixture was further stirred for 30 min in a 23-mL solvothermal vessel and was heated to 80 °C for 24 hrs. The product was collected by centrifugation, washed several times with ethanol and dried in air for characterization. We denote the synthesized Y(1,3,5-BTC)(nH_2O) as MOF-76(Y). FT-IR (KBr, 4000-400 cm^{-1}): 3435 (br), 2926 (w), 1670 (s), 1631 (s), 1616 (s), 1578 (m), 1541 (m), 1443 (s), 1379 (s), 1107 (w), 939 (w), 773 (m), 706 (m), 571 (w), 459 (w).

Synthesis of MOF-76(Y): Ln (Ln= Eu, Tb, Sm, Dy) and MOF-76(Y): x mol%Eu/y mol%Tb. A similar process was employed to prepare Y(1,3,5-BTC)(nH_2O): Ln, except for adding a certain amount of 10 mol% $Ln(NO_3)_3{\cdot}6H_2O$ (Ln = Eu, Tb, Sm, Dy) into the precursor solution at the initial stage, while other reaction parameters were kept unchanged. We denote the synthesized Y(1,3,5-BTC)(nH_2O): Ln as MOF-76(Y):Ln. Europium and terbium doped Y(1,3,5-BTC)(nH_2O) is also synthesized by a similar procedure, except for adding a certain amount of $Eu(NO_3)_3{\cdot}6H_2O$ and $Tb(NO_3)_3{\cdot}6H_2O$ into the precursor solution at the initial stage, while other reaction parameters were kept unchanged. The product was collected by centrifugation, washed several times with ethanol, and dried in air for characterization. We denoted the synthesized Eu^{3+} and Tb^{3+} substituted MOF as MOF-76(Y): x mol% Eu/y mol% Tb, (x mol% Eu^{3+}: y mol% Tb^{3+} = 1: 10, 5: 10, 10: 10, 10: 5, 10: 1).

Synthesis of nanosized MOF-76 (Y): Ln (Ln = Eu, Tb, Sm, Dy). A typical synthesis of nanosized Y(1,3,5-BTC)(nH_2O):Ln was as follows: a mixture of $Y(NO_3)_3{\cdot}6H_2O$ (0.107 g, 0.28 mmol), $Ln(NO_3)_3{\cdot}6H_2O$ (0.028 mmol), H_3BTC (0.020 g, 0.10 mmol) and $CH_3COONa{\cdot}3H_2O$ (0.027 g, 0.20 mmol) were dissolved in DMF (4 mL), and H_2O (3.2 mL) at room temperature. The mixture was further stirred for 30 min in a 23-mL solvothermal vessel and obtained white suspension liquid. And then, the precursor was heated to 80 °C for 24 hrs. The product was collected by centrifugation, washed several times with ethanol and dried in air for characterization. We denote the nanosized MOF-76 (Y): Ln as NMOF-76 (Y): Ln (Ln = Eu, Tb, Sm, Dy).

Synthesis of NMOF-76: Ln (Ln = Eu, Tb, Sm, Dy) polymer films. The transparent and luminescent MOF-76(Y):Ln polymer materials were prepared according to the procedure as follows: 10 mg NMOF-76:Ln was added into a flask with 1ml EMA and 10 mL THF. The mixture was further stirred for 30 min under 80 °C vacuum circumstances. The final luminescent polymer materials were finally prepared from the radical polymerization of the monomer ethyl methacrylate (EMA). Then, 0.0125 g BPO dissolved in 2 mL THF was added into the mixture and reacting 6 hrs. The THF was removed by rotary evaporation.

Characterization. Infrared spectra were measured within KBr pellets from 4000 to 400 cm^{-1} using a Nexus 912 AO446 Fourier transform infrared spectrum radiometer (FTIR). X-ray powder diffraction patterns (XRD) were acquired on Rigaku D/max-rB diffractometer equipped with Cu anode; the data were collected within the 2θ range of 5-65°. Thermogravimetric analysis (TG) was measure using a Netzsch STA 449C system at a heating rate of 5 °C/min under the nitrogen protection. The morphology of the samples was inspected using a scanning electron microscope (SEM, Philips XL-30). Energy Dispersive Analysis by X-rays (EDX) and transmission electron microscope (TEM) is carried out on a JEOL JEM-2010F electron microscope operated at 200 kV. The ultraviolet diffusion reflection spectra of the powdered samples were recorded by a B&WTEK BWS003 spectrophotometer. Luminescence excitation spectra and emission spectra were measured on an Edinburgh FLS920 fluorescence spectrometer. The lifetime measurements were measured on an Edinburgh Instruments FLS 920 fluorescence spectrometer using microsecond (100 mW) lamp. The outer luminescent quantum efficiency was determined using an integrating sphere (150 mm diameter, $BaSO_4$ coating) from Edinburgh FLS920 phosphorimeter. The spectra were corrected for variations in the output of the excitation source and for variations in the detector response. The quantum yield can be defined as the integrated intensity of the luminescence signal divided by the integrated intensity of the absorption signal. The absorption intensity was calculated by subtracting the integrated intensity of the light source with the sample in the integrating sphere from the integrated intensity of the light source with a blank sample in the integrating sphere. All of the measurements were performed at room temperature.

3. Results and Discussion

3.1 Structure, composition and morphology of MOF-76(Y) and MOF-76(Y): Ln (Ln = Eu, Tb, Sm, Dy)

A series of MOF-76(Y): Ln (Ln = Eu, Tb, Sm, Dy) were prepared and the typical coordination environment and structure of synthesized MOF-76(Y) are shown in Scheme 1. According to the reported literature[14b,16c], the structure of MOF-76(Y) is that the central Y is seven-coordinated by six oxygen atoms from the carboxylate groups of 1,3,5-BTC ligands to from a tetragonal porous framework of P_4322 space group.

Journal of Materials Chemistry C Accepted Manuscript

This journal is © The Royal Society of Chemistry 2012

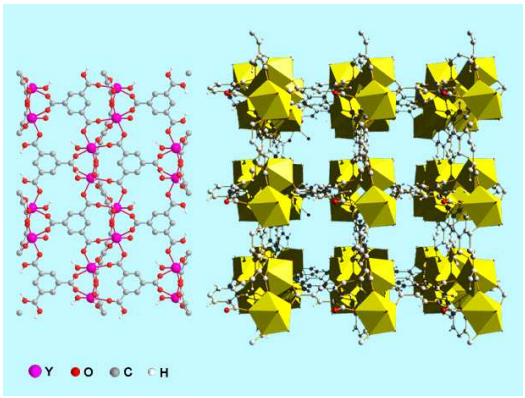

Scheme 1 The coordination environment of central atom Y (viewed from direction of (100) crystal plane) and the structure of MOF-76(Y).

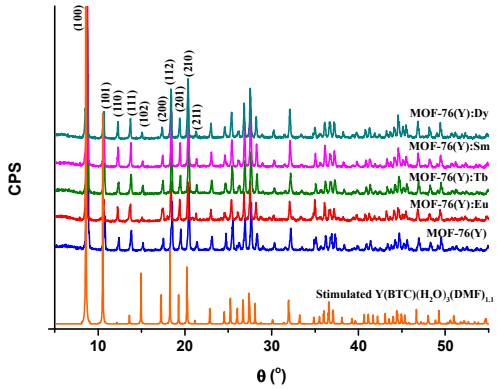

Fig. 1 XRD patterns of MOF-76(Y) and MOF-76(Y): Ln (Ln = Eu, Tb, Sm, Dy).

The X-ray powder diffraction (XRD) pattern of pure MOF-76(Y) exhibits several peaks in 2θ ranged 5-55 ° (Fig. 1), which matches pretty well with XRD pattern of stimulated $Y(BTC)(H_2O)_3(DMF)_{1.1}$[14b]. Furthermore, the structure of synthesized MOF-76(Y): Ln is also confirmed by XRD, which suggests the ordered porous structure of MOF-76(Y) is conserved after the introduction of lanthanide ions. The consistent XRD results indicate that introduction of doping lanthanide ions do not change the crystalline phase structure. However, compared to MOF-76(Y), it is worth noting that a slightly diffraction peak shift of lanthanide doping MOF is observed towards low diffraction angle (Table S1). Moreover, the crystalline interplanar spacing (d in Table S1) of all the materials can be obtained by Bragg equation, and analysis shows that the distance of crystal face of MOF increases by introducing lanthanide ions. This consequence can be attributed to the introduction of lanthanide into host lattice, which has larger atomic radius than yttrium. The element analysis of MOF-76(Y): Ln (Ln = Eu, Tb, Sm, Dy) are determined by EDX. From the EDX element analysis, it shows that the doping ratio of Ln (Ln = Eu, Tb, Sm, Dy) to Y are almost in accordance with the experiment doping mole ratio (Ln: Y= 0.1) (Table S2). We can also deduce that lanthanide ions are successfully incorporate into host lattice.

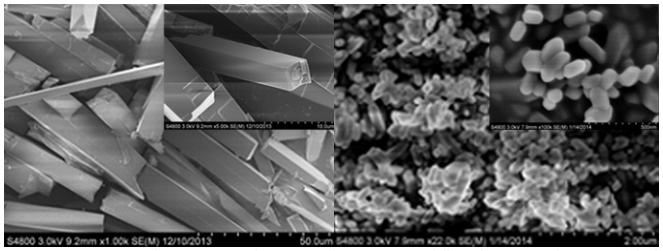

Fig. 2 SEM images of (A) low magnification and (a) high magnification of MOF-76(Y):Eu; (B) low magnification and (b) high magnification of NMOF-76(Y):Eu.

The morphology of crystals is studied by scanning electron micrograph. The rod-like structure of MOF-76(Y) does not change after ion substitution (Fig. S1). As shown in Fig. 2A, the sample of MOF-76(Y): Eu consists of relatively uniform rod-like crystals by using the solvothermal method at 80°C without chemical additives. A higher magnification SEM image (Fig. 2a) indicates that the crystal is regular square prism structure with the size of 10×10×80 μm^3. Fig. 2B shows images of obtained NMOF-76(Y): Eu, well-dispersed nanoparticles by introducing sodium acetate into precursor using solvothermal method at 80°C. Careful observation reveals that the obtained nanomaterial is like rice shape with the length of 150-250 nm and width of 100-150 nm (Fig. 2b). XRD patterns of resulting nanocrystals are nearly identical, indicating the unchanged XRD patterns of resulting nanocrystals are nearly identical, indicating the unchanged crystalline form (Fig. S2). The size reduction of MOF-76(Y): Eu is mainly due to the introducing of sodium acetate leading to the completive coordination, which is speculated to regulate the rate of crystal growth.

3.2 Lanthanide ions activated MOF-76(Y) materials with color tunable luminescence properties

3.2.1 Photoluminescence properties of MOF-76(Y): Ln

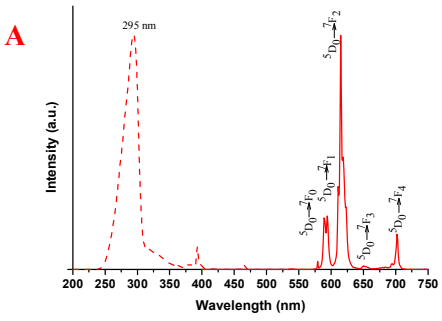

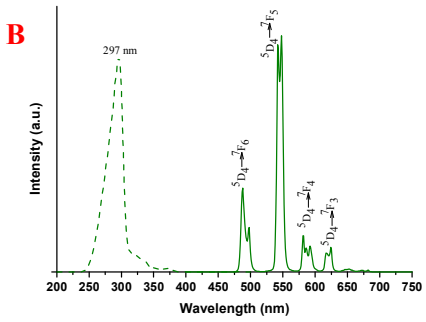

Journal of Materials Chemistry C Accepted Manuscript

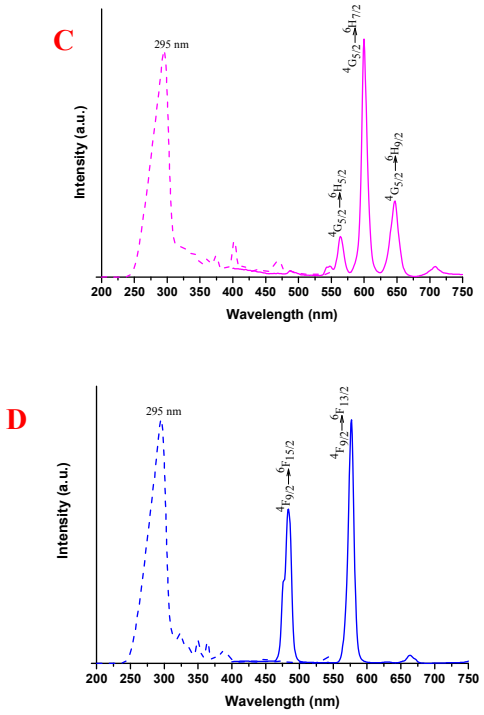

Fig. 3 Room temperature excitation and emission spectra of MOF-76(Y):Ln: Ln = Eu (A, λ_{ex} = 295 nm), Tb (B, λ_{ex} = 297 nm), Sm (C, λ_{ex} = 295 nm), Dy (D, λ_{ex} = 295 nm).

The emission spectrum of MOF-76(Y) exhibits a broad peak centered at 410 nm when it is excited by the wavelength of 315 nm (Fig. S3). Whereas, the emission spectra of ligand showed a broad peaks centered at 361 nm. The red shift of emission peak is probably because yttrium atom disturb the luminescence of 1,3,5-benzenetricarboxylic acid. The fluorescence excitation and emission spectra of the MOF-76(Y): Ln is displayed in Fig. 3. It is clearly showed from the figures that all the excitation spectra (the dashed line) dominated by a broad absorption bands located at ultraviolet region centered at about 295 nm, suggesting that the resulted materials can absorb the ultraviolet light efficiently and then sensitize the emission of lanthanide by energy transfer. The luminescence of MOF-76(Y):Ln is mainly attributed to the organic ligand's excited energy levels with a subsequent transfer to the resonant excited levels of lanthanide ions, and therefore yielding a final strong light emission. Furthermore, the emission spectra (the solid line) of MOF-76(Y): Ln are obtained by using appropriate wavelength as excitation source, which display their characteristic emission peaks. The emission lines of MOF-76(Y):Eu are assigned to $^5D_0\rightarrow 7F_0$, $^5D_0\rightarrow 7F_1$, $^5D_0\rightarrow^7F_2$, $^5D_0\rightarrow^7F_3$ and $^5D_0\rightarrow^7F_4$ transitions for those peaks located at about 579, 594, 615, 651, and 702 nm, respectively. It can be observed that the emission spectra shown in Fig.3A are dominated by a very intense $^5D_0\rightarrow^7F_2$ transition at 616 nm. It is well known that the $^5D_0\rightarrow^7F_2$ transition is a typical electric dipole transition and is very sensitive to the local symmetry of europium ions, while the parity-allowed magnetic dipole transition $^5D_0\rightarrow^7F_1$ is practically independent of the ions' surroundings. Hence, the intensity ratios $I(^5D_0\rightarrow^7F_2)/I(^5D_0\rightarrow^7F_1)$ (I_{02}/I_{01}) can be seen as an indicator for the local environment of ions. According to the calculated intensity ratio for 3.6, we concluded that the chemical environment around the europium ions is in low symmetry. For MOF-76(Y): Tb, the emission lines depicted on the right of Fig. 3B are assigned to $^5D_4\rightarrow^7F_6$, $^5D_4\rightarrow^7F_5$, $^5D_4\rightarrow^7F_4$ and $^5D_4\rightarrow^7F_3$ transitions for those peaks located at 488, 548, 582 and 624 nm, respectively. The emission peaks of MOF-76(Y): Sm are assigned to $^4G_{5/2}\rightarrow^6H_{5/2}$, $^4G_{5/2}\rightarrow^6H_{7/2}$ and $^4G_{5/2}\rightarrow^6H_{9/2}$ transitions for those peaks located at 564, 600, and 647 nm, respectively (Fig. 3C). For MOF-76(Y): Dy, the emission lines depicted on the right of Fig. 3D are assigned to $^4F_{9/2}\rightarrow^6F_{15/2}$ and $^4F_{9/2}\rightarrow^6F_{13/2}$ transitions for those peaks located at 484 and 577 nm, respectively. Furthermore, the UV–vis diffuse reflectance spectra of MOF-76(Y): Ln is in accordance with emission spectra. Adsorption bands observed in Fig.S4 indicate that the 1,3,5-benzenetricarboxylic acid ligands absorb the ultraviolet light centered at 293 nm. Then, all the lanthanide ions doped MOF-76(Y) are expected to have excellent photoluminescence properties under the irradiation of ultraviolet light, which has been proved in the luminescence spectra (Fig. 3). In addition, the peaks in UV-Vis diffuse reflectance spectra at 616 nm appearing in MOF-76(Y):Eu can be ascribed to $^5D_0\rightarrow^7F_2$, and peaks at 546 nm in MOF-76(Y):Tb can be assigned to $^5D_4\rightarrow^7F_5$.

Table 1 The luminescent efficiencies and lifetimes for MOF-76: Ln (Ln = Eu, Tb, Sm, Dy).

Materials	τ (μs)[a]	η (%)[b]
MOF-76(Y): Eu	704	82%
MOF-76(Y): Tb	1460	91%
MOF-76(Y): Sm	14	4%
MOF-76(Y): Dy	14	18%

[a] lifetimes (τ) of $^5D_0$ energy level for Eu^{3+} excited state, $^5D_4$ energy level for Tb^{3+} excited state, $^4G_{5/2}$ energy level for Sm^{3+} excited state, $^4H_{9/2}$ energy level for Dy^{3+} excited state, respectively; [b] the luminescent quantum efficiencies are measured on an Edinburgh Instruments FLS 920 fluorescence spectrometer.

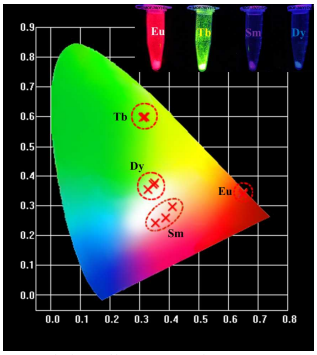

Fig. 4 CIE x-y chromaticity diagram of MOF-76(Y): Ln (Ln=Eu, Tb, Sm, Dy) with different doping ratio (1 mol%, 5 mol% 10 mol%) using the excitation wavelength of 300 nm. The insert is MOF-76(Y): Ln under the excitation wavelength of 254 nm.

For further investigation of the photoluminescence properties, we measure the luminescence lifetime decay curves of MOF-76: Ln at room temperature, the resulting lifetimes are given in Table 1. Besides, we measure efficiencies on an Edinburgh Instruments FLS 920 fluorescence spectrometer and the resulting emission quantum efficiencies are listed in Table 1.

Journal of Materials Chemistry C Accepted Manuscript

This journal is © The Royal Society of Chemistry 2012

As displayed in Table 1, MOF-76(Y): Eu and MOF-76(Y): Tb possess much higher quantum efficiencies than MOF-76(Y): Sm and MOF-76(Y): Dy. As illustrated in Fig. 4, the CIE chromaticity coordinates for MOF-76: Ln fall in red-orange, green-yellow, pink, and light green, respectively. Under 300 nm excitation, MOF-76(Y): Eu and MOF-76(Y): Tb both show fairly bright. However, the luminescence of MOF-76(Y): Sm and MOF-76(Y): Dy is comparatively weak. It might be due to unmatchable energy level between the triple excitation state of benzenetricarboxylic acid and the excitation energy level of Sm^{3+} or Dy^{3+}. Therefore, changing the doping ratio hardly causes moving of coordinates of MOF-76(Y): Eu or MOF-76(Y): Tb, which remain the bright luminescence of red or green. When it comes to MOF-76(Y): Dy or MOF-76(Y): Sm, different doping ratio (1 mol%, 5 mol% 10 mol%) causes slightly shift of coordinates. With the decrease of doping concentration of Sm^{3+} or Dy^{3+}, the coordinates gradually move towards the blue region.

3.2.2 Photoluminescence properties of MOF-76(Y): x mol% Eu/y mol% Tb

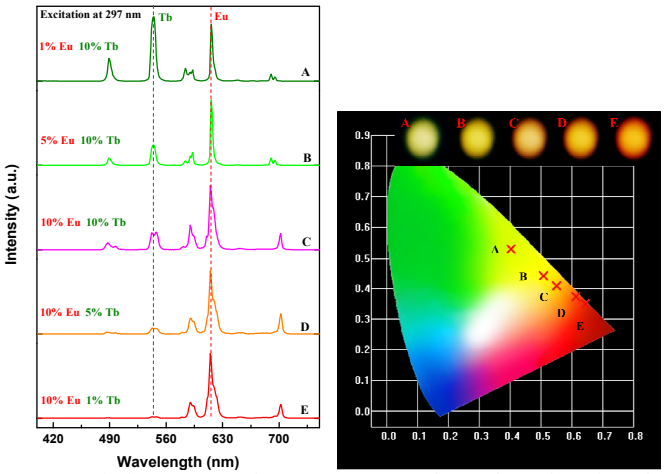

Fig. 5 Emission spectra of MOF-76(Y):x mol% Eu/y mol% Tb under the excitation of 297 nm and CIE x-y chromaticity diagram of MOF-76(Y): x mol% Eu/y mol% Tb. (A) MOF-76(Y): 1 mol% Eu/10 mol% Tb; (B) MOF-76(Y): 5 mol% Eu/10 mol% Tb; (C) MOF-76(Y): 10 mol% Eu/10 mol% Tb; (D) MOF-76(Y): 10 mol% Eu/5 mol% Tb; (E) MOF-76(Y): 10 mol% Eu/1 mol% Tb.

Obtained Eu^{3+} and Tb^{3+} ions co-activated MOF-76(Y) has the same morphology and crystallinity with MOF-76(Y). Fig. 5 shows the emission spectra of the co-doped MOF-76(Y): x mol% Eu/y mol% Tb under 297 nm excitation (the maximum excitation wavelength of MOF-76: Eu and MOF-76: Tb). The concentration of europium and terbium are 1 mol% Eu/10 mol% Tb, 5 mol% Eu/10 mol% Tb, 10 mol% Eu/10 mol% Tb, 10 mol% Eu/5 mol% Tb, and 10 mol% Eu/1 mol% Tb, which giving emission of yellow-green, yellow, warm yellow, orange, and red, respectively. Even with a minimal Eu content of 1 mol% in MOF-76(Y):1 mol% Eu/10 mol% Tb, the characteristic emission peak at 616 nm attribute to $^5D_0 \rightarrow {}^7F_2$ transition within Eu^{3+} is detectable with considerable intensity. Under 297 nm excitation, it yields the characteristic emissions of the Eu^{3+} and Tb^{3+} ions. When the doping concentration of europium increases, it can be observed a significant change in relatively intensity of green emission of Tb^{3+} in MOF-76(Y), which decreases strongly along with the raised mole ratio of europium. Besides, the emission of Tb is almost absent while the Eu^{3+} concentration is 10 mol% and Tb^{3+} 1 mol%. However, the increasing doping ratio of Tb^{3+} does not have a great influence on the emission of Eu^{3+}. For further study of luminescence mechanism, we investigate lifetime of Eu^{3+} ($^5D_0 \rightarrow {}^7F_2$) and Tb^{3+} ($^5D_4 \rightarrow {}^7F_5$) in MOF-76(Y):x mol% Eu/y mol% Tb under 297 nm excitation (Table S3). It clearly shows that the lifetime of Eu^{3+} ($^5D_0 \rightarrow {}^7F_2$) and Tb^{3+} ($^5D_4 \rightarrow {}^7F_5$) do not change much when the concentration of Eu^{3+} and Tb^{3+} varies. Therefore, the results indicate that there is no energy transfer phenomenon between Eu^{3+} and Tb^{3+}, which may probably due to the distance between Eu atom and Tb atom are relatively far, leading to the difficulty to energy transfer. We also co-doped Sm and Tb into MOF-76(Y), which is denoted as MOF-76(Y):x mol% Sm/y mol% Tb(x: y = 1: 10, 5: 10, 10: 10, 10: 5, 10: 1) (Fig. S5). Since the emission of samarium is comparatively weak, the CIE coordinates of MOF-76(Y):x mol% Sm/y mol% Tb are all located in yellow-green area, which is resulted from dominant luminescence of terbium ions.

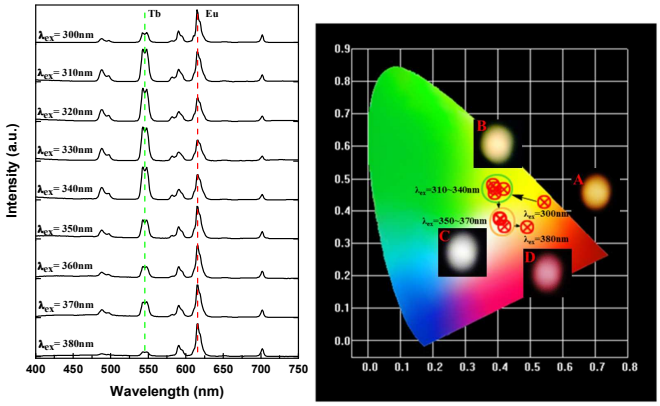

Fig. 6 Emission spectra of MOF-76(Y):10 mol% Eu/10 mol% Tb under the excitation ranged from 300-380 nm and CIE x-y chromaticity diagram of MOF-76(Y):10 mol% Eu/10 mol% Tb under different excitation wavelength. The inserts shows luminescence of 10 mol% Eu/10 mol% Tb under the excitation of (A) 300 nm, (B) 330 nm, (C) 360 nm, and (D) 380 nm.

Interestingly, the photoluminescence color of MOF-76(Y):10 mol% Eu/10 mol% can be tuned from yellow, yellow-green, warm white to orange by changing excitation wavelength from 300-380 nm. Fig. 6 shows the corresponding CIE chromaticity diagram of MOF-76(Y):10 mol% Eu/10 mol% Tb under different excitation wavelength (300-380 nm). There is a little difference between the excitation spectra monitored by 616 nm (Eu^{3+}: $^5D_0 \rightarrow {}^7F_2$) and 548 nm ($Tb^{3+}$: $^5D_4 \rightarrow {}^7F_5$). As showed in Fig. S6, the excitation band of Tb^{3+} ranged from 250-350 nm is quite broader than Eu^{3+} from 250 to 310 nm, in the meanwhile, there is a excitation line centered at 392 nm in the excitation monitored by 616 nm (Eu^{3+}: $^5D_0 \rightarrow {}^7F_2$). Therefore, when wavelength changed from 300 nm to 380 nm, the different energy absorbing trend of Eu^{3+} and Tb^{3+} yields various photoluminescence color.

3.3 The luminescence of NMOF-76:Ln (Ln = Eu, Tb, Sm, Dy) polymer film

Journal of Materials Chemistry C Accepted Manuscript

The SEM image of NMOF-76: Eu fabricated polymer film is shown in Fig. 7. The film surface is smooth, continuous, and defect free over a large area. The XRD pattern of NMOF-76(Y):Ln fabricated in polymer film is shown in Fig. S7. Since NMOF-76:Eu is physically dispersed in polymer host, in which polymer host is large amount and NMOF-76:Eu is little amount. So the broad diffraction peaks in its XRD pattern are dominated by the amorphous state of polymer host materials are amorphous. While the diffraction peaks for crystal phase of NMOF-76:Eu cannot be seen very clearly for its limited amount in the polymer host. The IR spectra of NMOF-76(Y):Eu displays the retained peaks centered at 1610 cm^{-1} and 1440 cm^{-1}, which means unchanged coordination form of H_3BTC and lanthanide ions (Fig. S8). The fluorescence excitation and emission spectra of the NMOF-76(Y): Ln polymer films are showed in Fig. S9. Excitation spectra of NMOF-76(Y): Ln polymer films are quite similar with powder MOF-76(Y): Ln, the absorption band of which centered at 295 nm. Since poly(methyl methylacrylate) (PEMA) acts as a physical matrix, polymerization reaction does not change the photoluminescence mechanism, that is, organic ligand's excited energy levels with a subsequent transfer to the resonant excited levels of lanthanide ions yielding a light emission. Both NMOF-76(Y): Eu and NMOF-76(Y):Tb fabricated polymer films show their characteristic transition emission (red and green color) under 295 nm excitation. The intensity ratio between electric dipole transition and magnetic dipole transition, $I(^5D_0 \rightarrow {}^7F_2)/I(^5D_0 \rightarrow {}^7F_1)$ (I_{02}/I_{01}), is 3.8 in NMOF-76(Y):Eu polymer film compared to 3.6 in the powder MOF-76(Y):Eu. It can be deduced that coordination environment of Eu^{3+} does not change much after polymerization, which is also in low symmetry coordination environment. While NMOF-76(Y): Sm and NMOF-76(Y):Dy fabricated polymer films present relatively weak luminescence. It can be observed that, besides the characteristic emission lines of Sm^{3+} and Dy^{3+}, there is a broad band located in 400-500 nm, which can be attributed to the luminescence of polymer matrix. NMOF-76(Y): Ln polymer films are transparent under the sunlight (Fig. 7B1), while showing emission of red, green, pink and cold white in the ultraviolet box (254 nm excitation) (Fig. 7B2).

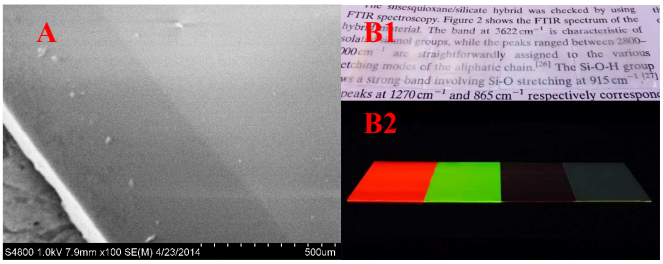

Fig. 7 (A) SEM image of NMOF-76:Eu polymer film; Images of the NMOF-76:Ln (Ln=Eu, Tb, Sm, Dy) polymer film (B1) under sunlight and (B2) in the ultraviolet box (under 254 nm excitation).

Conclusions

Novel lanthanide (Eu, Tb, Sm, Dy) ions doped yttrium 1,3,5-benzenetricarboxylate have been prepared via solvothermal method. Fluorescence spectra indicates that MOF-76(Y): Ln (Ln = Eu, Tb, Sm, Dy) reveal characteristic emission lines under ultraviolet radiation. The tunable color luminescence property of europium and terbium co-doped yttrium 1,3,5-benzenetricarboxylate is depending on the dopant concentration of europium and terbium and on excitation wavelength. Moreover, the lanthanide ions doped MOF-76(Y) polymer film can be obtained via embedding nanosized MOF-76(Y): Ln into PEMA. The resulting transparent hybrid materials can be used in the fabrication of different plastic photonic devices.

Acknowledgements

This work was supported by the National Natural Science Foundation of China (91122003), Program for New Century Excellent Talents in University (NCET 2008-08-0398).

Notes and references

[a] Department of Chemistry, Tongji University; State Key Lab of Water Pollution and Resource Reuse (Tongji University), Siping Road 1239, Shanghai 200092, China. Fax: +86-21-65982287; Tel: +86-21-65984663; E-mail: byan@tongji.edu.cn

† Footnotes should appear here. These might include comments relevant to but not central to the matter under discussion, limited experimental and spectral data, and crystallographic data.

Electronic Supplementary Information (ESI) available: [details of any supplementary information available should be included here]. See DOI: 10.1039/b000000x/

References

1. (*a*) X. Duan, J. C. Yu, J. F. Cai, Y. B. He, C. D. Wu, W. Zhou, T. Yildirim, Z. J. Zhang, S. C. Xiang, M. O'Keeffe, B. L. Chen and G. D. Qian, *Chem. Commun.*, 2013, **49**, 2043-2045; (*b*) Y. B. He, Z. Y. Guo, S. C. Xiang, Z. J. Zhang, W. Zhou, F. R. Fronczek, S. Parkin, S. T. Hyde, M. O'Keeffe and B. L. Chen, *Inorg. Chem.*, 2013, **52**, 11580-11584; (*c*) Y. Hu, Z. X. Liu, J. Xu, Y. N. Huang and Y. Song, *J. Am. Chem. Soc.*, 2013, **135**, 9287-9290; (*d*)
2. (*a*) C. Y. Sun, C. Qin, X. L. Wang and Z. M. Su, *Expert. Opin. Drug. Del.*, 2013, **10**, 89-101; (*b*) J. S. Qin, D. Y. Du, W. L. Li, J. P. Zhang, S. L. Li, Z. M. Su, X. L. Wang, Q. Xu, K. Z. Shao and Y. Q. Lan, *Chem. Sci.*, 2012, **3**, 2114-2118; (*c*) Y. Wang, J. Yang, Y. Y. Liu and J. F. Ma, *Chem. Eur. J.*, 2013, **19**, 14591-14599.
3. (*a*) Z. M. Hao, X. Z. Song, M. Zhu, X. Meng, S. N. Zhao, S. Q. Su, W. T. Yang, S. Y. Song and H. J. Zhang, *J. Mater. Chem. A.*, 2013, **1**, 11043-11050; (*b*) L. E. Kreno, K. Leong, O. K. Farha, M. Allendorf, R. P. Van Duyne and J. T. Hupp, *Chem. Rev.*, 2012, **112**, 1105-1125; (*c*) J. M. Zhou, W. Shi, N. Xu and P. Cheng, *Inorg. Chem.*, 2013, **52**, 8082-8090.
4. (*a*) A. Dhakshinamoorthy, M. Alvaro and H. Garcia, *Chem. Commun.*, 2012, **48**, 11275-11288; (*b*) J. L. Wang, C. Wang and W. B. Lin, *Acs. Catal.*, 2012, **2**, 2630-2640.
5. (*a*) J. H. Cui, Y. Z. Li, Z. J. Guo and H. G. Zheng, *Chem. Commun.*, 2013, **49**, 555-557; (*b*) Z. Jin, H. Y. Zhao, D. J. Yang, X. D. Yao and G. S. Zhu, *Inorg. Chem. Commun.*, 2012, **25**, 74-78; (*c*) J. H. Cui, Z. Z. Lu, Y. Z. Li, Z. J. Guo and H. G. Zheng, *Chem. Commun.*, 2012, **48**, 7967-7969.

Journal of Materials Chemistry C Accepted Manuscript

This journal is © The Royal Society of Chemistry 2012

6. (*a*) C. R. Wade, M. Y. Li and M. Dinca, *Angew. Chem. Int. Edit.*, 2013, **52**, 13377-13381; (*b*) Y. P. Miao, B. Liu, K. L. Zhang, H. Zhang, R. Wang, Y. Liu and J. Q. Yao, *Opt. Laser. Technol.*, 2013, **48**, 280-284; (*c*) P. Falcaro and S. Furukawa, *Angew. Chem. Int. Edit.*, 2012, **51**, 8431-8433.
7. (*a*) J. C. Yu, Y. J. Cui, H. Xu, Y. Yang, Z. Y. Wang, B. L. Chen and G. D. Qian, *Nat. Commun.*, 2013, **4**; (*b*) J. Della Rocca, D. M. Liu and W. B. Lin, *Accounts. Chem. Res.*, 2011, **44**, 957-968.
8. M. D. Allendorf, C. A. Bauer, R. K. Bhakta and R. J. T. Houk, *Chem. Soc. Rev.*, 2009, **38**, 1330-1352.
9. (*a*) S. K. Ghosh, J. P. Zhang and S. Kitagawa, *Angew. Chem. Int. Edit.*, 2007, **46**, 7965-7968; (*b*) T. K. Maji, G. Mostafa, H. C. Chang and S. Kitagawa, *Chem. Commun.*, 2005, **19**, 2436-2438. (*c*) M. J. Vitorino, T. Devic, M. Tromp, G. Férey and M. Visseaux, *Macromol. Chem. Phys.*, 2009, **210**, 1923-1932.
10. (*a*) K. A. White, D. A. Chengelis, K. A. Gogick, J. Stehman, N. L. Rosi and S. Petoud, *J. Am. Chem. Soc.*, 2009, **131**, 18069-18071; (*b*) J. Rocha, L. D. Carlos, F. A. A. Paz and D. Ananias, *Chem. Soc. Rev.*, 2011, 40, 926-940; (c) E. F. de Melo, N. D. C. Santana, K. G. B. Alves, G. F. de Sá, C. P. de Melo, M. O. Rodrigues and S. A. Júnior, *J. Mater. Chem. C.*, 2013, **1**, 7574-7581.
11. (*a*) M. Ma, D. Zacher, X. N. Zhang, R. A. Fischer and N. Metzler-Nolte, *Cryst. Growth. Des.*, 2011, **11**, 185-189; (*b*) A. Ranft, S. B. Betzler, F. Haase and B. V. Lotsch, *Crystengcomm.*, 2013, **15**, 9296-9300; (*c*) A. Kondo, C. C. Tiew, F. Moriguchi and K. Maeda, *Dalton. T.*, 2013, **42**, 15267-15270; (*d*) G. Xu, T. Yamada, K. Otsubo, S. Sakaida and H. Kitagawa, *J. Am. Chem. Soc.*, 2012, **134**, 16524-16527.
12. (*a*) A. Centrone, Y. Yang, S. Speakman, L. Bromberg, G. C. Rutledge and T. A. Hatton, *J. Am. Chem. Soc.*, 2010, **132**, 15687-15691; (*b*) E. Y. Choi, C. Gao, H. J. Lee, O. P. Kwon and S. H. Lee, *Chem. Commun.*, 2009, 7563-7565; (*c*) S. S. Mondal, A. Bhunia, S. Demeshko, A. Kelling, U. Schilde, C. Janiak and H. J. Holdt, *Crystengcomm.*, 2014, **16**, 39-42.
13. (*a*) K. M. Gupta, Y. F. Chen and J. W. Jiang, *J. Phys. Chem. C.*, 2013, **117**, 5792-5799; (*b*) E. Redel, Z. B. Wang, S. Walheim, J. X. Liu, H. Gliemann and C. Woll, *Appl. Phys. Lett.*, 2013, **103**, 091903.
14. (*a*) R. Ma, H. Chu, Y. Zhao, Q. Wuren and M. Shan, *Spectrochim. Acta. A.*, 2010, **77**, 419-423; (*b*) H. L. Jiang, N. Tsumori and Q. Xu, *Inorg. Chem*, 2010, **49**, 10001-10006; (*c*) H. H. Song, F. Yang, J. Y. Wang and S. K. Shi, *Spectrosc. Spect. Anal*., 2007, **27**, 2093-2097.
15. N. L. Rosi, J. Kim, M. Eddaoudi, B. L. Chen, M. O'Keeffe and O. M. Yaghi, *J. Am. Chem. Soc.*, 2005, **127**, 1504-1518.
16. (*a*) K. Liu, H. P. You, Y. H. Zheng, G. Jia, Y. H. Song, Y. J. Huang, M. Yang, J. J. Jia, N. Guo and H. J. Zhang, *J. Mater. Chem.*, 2010, **20**, 3272-3279; (*b*) B. L. Chen, Y. Yang, F. Zapata, G. N. Lin, G. D. Qian and E. B. Lobkovsky, *Adv. Mater.*, 2007, **19**, 1693-1696; (*c*) J. H. Luo, H. W. Xu, Y. Liu, Y. S. Zhao, L. L. Daemen, C. Brown, T. V. Timofeeva, S. Q. Ma and H. C. Zhou, *J. Am. Chem. Soc.*, 2008, **130**, 9626-9627.
17. (*a*) B. L. Chen, L. B. Wang, F. Zapata, G. D. Qian and E. B. Lobkovsky, *J. Am. Chem. Soc.*, 2008, **130**, 6718-6719; (*b*) T. Lee, H. L. Lee, M. H. Tsai, S. L. Cheng, S. W. Lee, J. C. Hu and L. T. Chen, *Biosens. Bioelectron.*, 2013, **43**, 56-62; (*c*) W. T. Yang, Z. Q. Bai, W. Q. Shi, L. Y. Yuan, T. Tian, Z. F. Chai, H. Wang and Z. M. Sun, *Chem. Commun.*, 2013, **49**, 10415-10417.

Journal of Materials Chemistry C Accepted Manuscript

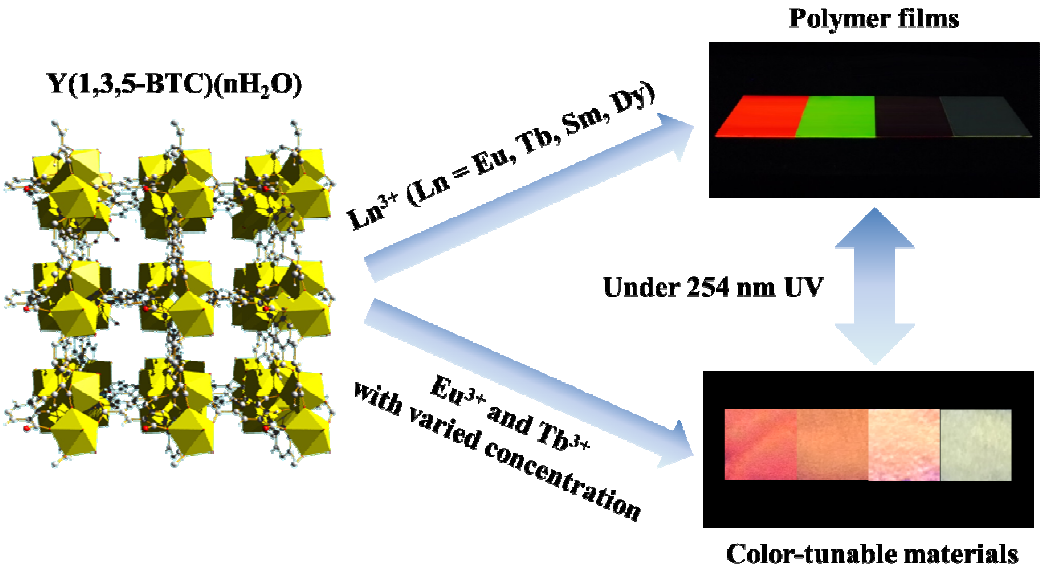

A series of novel lanthanide (Eu, Tb, Sm, Dy) doped yttrium 1,3,5-benzenetricarboxylate have been obtained via solvo-thermal method. The synthesized polymer films of obtained materials extend the application fields in fabricating plastic photonic devices. With varied concentration of co-doped europium and terbium in yttrium 1,3,5-benzenetricarboxylate, the emitting colors of obtained materials changed under the same excitation wavelength.

Journal of Materials Chemistry C Accepted Manuscript